Drop-Size Distributions Associated with Intense Rainfall

PAUL T. WILLIS

Atlantic Oceanographic and Meteorological Laboratory, Miami, Florida

PAUL TATTELMAN

Air Force Geophysics Laboratory, Hanscom Air Force Base, Massachusetts

(Manuscript received 24 October 1987, in final form 2 March 1988)

ABSTRACT

The probability of occurrence of extreme rainfall rates is reviewed. The drop-size distributions associated with a range of high rainfall rates are examined using data from tropical storms and hurricanes. Mean drop-size distributions are presented for a range of high rainfall rates, as well as a Γ-distribution fit to the entire set of normalized drop-size distributions. This fit forms the basis for a model drop-size distribution for intense rain. The goodness of fit of the model is examined by comparing it with independent drop-camera measurements of high-rain-rate distributions from several geographic locations. The slope of exponential fits to the distributions are examined for constancy with rainfall rate, and are generally found to decrease with increasing rainfall rate.

1. Introduction

The distributions of hydrometeors at the surface and aloft associated with extreme rainfall rates are important from an engineering, scientific, and climatological point of view. The design and operation of many types of equipment, particularly aerospace systems, are sensitive to the presence of hydrometeors. Impaction with precipitation particles often entails a potential for damage or failure. Communication systems, particularly those using microwave frequencies, are sensitive to the details of hydrometeor extremes. The raindrop size distributions in intense rainfall are important for the scientific assessment of the roles of drop breakup and coalescence in shaping the distributions at all rainfall rates. Details of the size distributions are particularly important to the measurement of precipitation rate by radar and other remote sensing techniques. Drop-size distributions associated with extreme rainfall rates are important to the fundamental scientific study of precipitation physics, as well as having important practical application to many facets of equipment engineering design.

In spite of their importance, studies of drop-size distributions in intense rainfall have not been numerous. In a survey of drop-size data at high rainfall rates, Blanchard and Spencer (1970) conclude that only the studies of Mueller and Sims (1966) and Hudson (1963) include extensive data at intensities > 100 mm h^{-1}. The purpose of this study is to present a new set of drop-size distributions in intense rainfall and develop a model for describing these distributions for practical applications. These new high-intensity rain data were observed during aircraft research and reconnaissance of Atlantic hurricanes and tropical storms. The new data are compared with previous results by Mueller and Sims, and a climatological perspective is developed.

2. Extreme rainfall rates

For design considerations that involve rain, it is necessary to know probabilities of extreme rates at locations that are noted for heavy rain. Although rainfall amounts are available for thousands of locations worldwide, data collection has been oriented toward agricultural and hydrological purposes for which monthly, daily, and, less commonly, 3 and 6 h totals are collected. But, for engineering design considerations much-shorter-time rain rates are appropriate. Since 1-min rain rates are most practical for engineering design, a regression model for estimating 1-min rates was developed (Tattelman and Scharr 1983). This model can be used to determine the monthly frequency of 1-min rates at locations for which routine climatological data are available.

Atlases of 1-min rates based on the Tattelman-Scharr model (Tattelman and Grantham 1983a,b) were used to determine the areas in the world with the highest rainfall rates occurring 0.5%, 0.1%, and 0.01% of the time during the rainiest month. Although rates are generally highest in the Northern Hemisphere tropics, the estimated rates for two locations in northeast Brazil, Barro Do Corda, and Teresina, are about the same as the rates estimated for Cherrapunji, India, a location

Corresponding author address: Mr. Paul T. Willis, NOAA/AOML, Hurricane Research Division, Miami, FL 33149.

known for heavy rain. The rates for this area in northeast Brazil are 36 mm h^{-1}, 84 mm h^{-1}, and 168 mm h^{-1} for 0.5%, 0.1%, and 0.01% of the rainiest month, respectively.

Elsewhere in the Northern Hemisphere tropics rates exceed 24, 72, and 144 mm h^{-1} during 0.5%, 0.1%, and 0.01% of the rainiest month in many areas, especially in southeast Asia. Since these rates occur over large areas in the tropics, the slightly higher rates in northeastern Brazil are recommended as representing the rainiest month/worst area rates.

By comparison, the 1-min and 1-h world record rates are 1872 mm h^{-1} and 432 mm h^{-1}, respectively. The 1-min record was recorded at Unionville, Maryland, on 4 July 1956. The 1 h record, which actually fell in 42 min, was recorded at Holt, Missouri, on 22 June 1947.

3. Drop-size distributions

a. Instrumentation and data

The new data used to specify drop-size distributions are from hurricanes and tropical storms that occurred from 1975–1982. They were collected by an optical spectrometer system described by Knollenberg (1981). We obtained the data studied herein with the precipitation probe, which has a 32-element photodiode array covering diameters from 100–6500 μm with 200 μm resolution, or spacing between the elements. We present data from 10 s summations, which cover horizontal distances from 0.9–1.5 km, depending upon the true air speed, which is a function of the aircraft used and the altitude flown. Ordinarily, the 10 s sample encompasses a volume of about 2 m^3. Any probe overload condition decreases this, but, during overload conditions the total number of drops sampled is very high. The data were machine-reduced objectively, using software described by Jorgensen and Willis (1982).

The high-intensity rainfall dataset used in this study was extracted from approximately 14 000 10 s aircraft samples in nonzero rainfall rate ($R > 0$). The bulk of the data were sampled at two altitudes, 450 and 3000 m. A small sample was obtained at two additional altitudes, the first at 150 m, and the second between the two primary sampling altitudes at 1500 m. The results are compared with the Mueller and Sims data, which were taken with a drop camera during 1 yr periods at several locations around the world. These cubic meter samples, each covering 10.5 s, were taken at 1 min intervals.

Since several hundred individual spectra cannot be presented here, the data were stratified by four rainfall rate categories (25–62.5, 62.5–125, 125–225, and >225 mm h^{-1}) and two sampling altitudes (3000 and 450 m). Then they were bin-averaged for each 200 μm diameter interval. The resultant drop-size distributions for each of the four rainfall rate stratifications are shown in Fig. 1 for the entire dataset. Also plotted in Fig. 1 is a Γ-distribution fit discussed below in section 3b. The data for each of the two primary sampling altitudes, stratified using the same rate intervals, are presented in Figs. 2–3 (no rates > 225 mm h^{-1} were in the 3000 m data).

The primary difference in spectral shape between the two altitudes is the greater tendency towards bimodality in the distributions sampled at 450 m. This tendency, though present at both altitudes, is enhanced at the lower altitude at the higher rainfall rates. This is possibly due to the fact that the processes forming the raindrop distribution, viz. the balance between coalescence growth and drop breakup, has more time at the lower level to approach an equilibrium condition. It is premature to compare these observed spectra to theoretically developed distributions, e.g., Valdez and Young (1985). The 450-m sample also appears to be characterized by fewer small drops than the high level sample. Although one might expect a better-developed drop-breakup process at lower levels to produce more small drops, apparently the coalescence process is efficiently removing these small drops. Also, if these high-rate spectra are associated with downdrafts, evaporation could be depleting the small raindrops and cloud droplets.

The entire set of high-intensity rainfall data was normalized after the method of Sekhon and Srivastava (1970, 1971) to remove dependence of the distribution upon water content or rainfall rate (Fig. 4). The data points are tightly grouped in the middle range of drop diameters. A curvilinear least-squares–fit routine is then used to fit to the entire set of data points ($R > 25$ mm h^{-1}, $N = 4624$ points); this fit forms the basis for the drop-distribution model proposed subsequently.

b. Drop-size distribution model

Blanchard and Spencer (1970) indicate that a given high-intensity rainfall rate might correspond to a particular drop-size distribution, where drop growth is balanced by drop breakup. They hypothesize that the drop-size distribution in heavy rain is the same, whether it originates from marine shower clouds or continental thunderstorms. They found that as the rain intensity exceeded 100 mm h^{-1}, the largest drops in the distributions did not continue to increase in size relative to the smaller drops. Instead, as the rain intensity continued to increase, the total number of drops continued to increase. In our data from flight levels well below the freezing level, we do not find extremely large-diameter drops ($D > 5$ mm) at the very high rainfall rates. There is some indication that the maximum sizes stabilize, or even decrease slightly, at the highest rates. The large drops are difficult to observe adequately because of their low concentrations and the small spatial scale of high-intensity rain. However, for high-intensity rain we definitely observe significantly lower concentrations of drops of diameter greater than 4 mm than would be indicated by the Marshall-Palmer (Marshall and Palmer 1948) distributions.

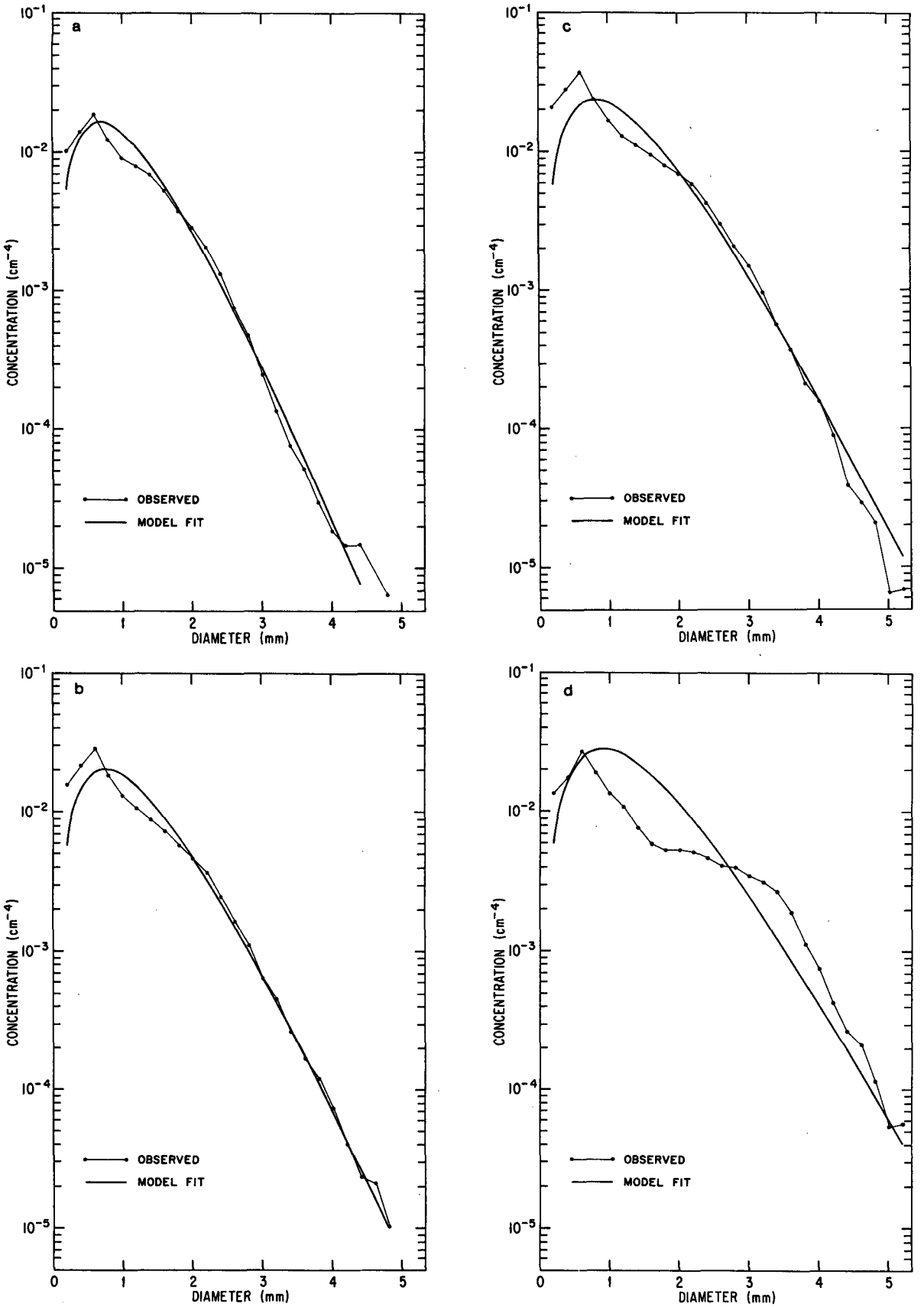

FIG. 1. Mean drop-size distributions from observations at all altitudes, and Γ-function fit, for rain rates: a) 25–62.5 mm h^{-1}, b) 62.5–125 mm h^{-1}, c) 125–225 mm h^{-1}, and d) >225 mm h^{-1}.

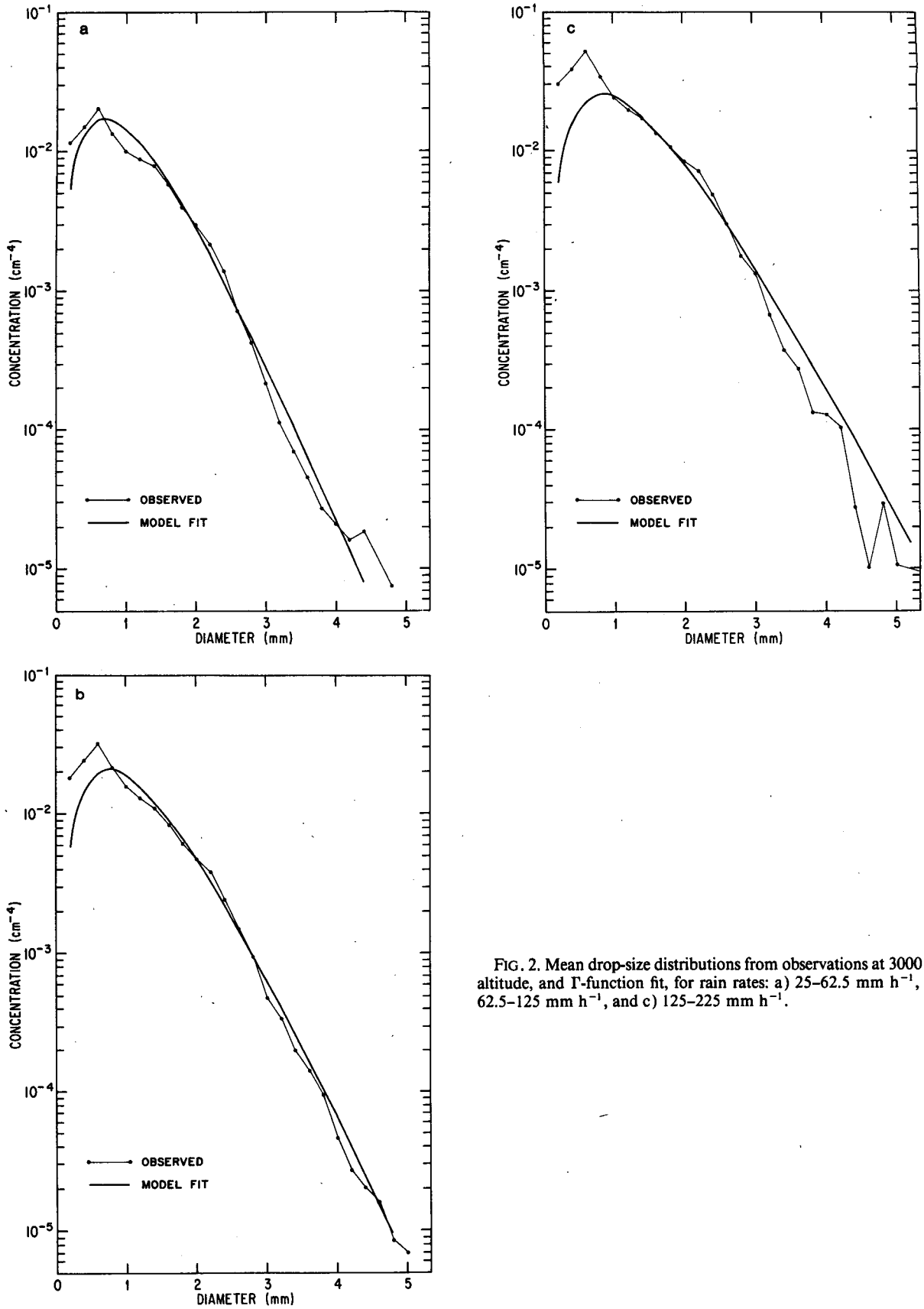

FIG. 2. Mean drop-size distributions from observations at 3000 m altitude, and Γ-function fit, for rain rates: a) 25–62.5 mm h^{-1}, b) 62.5–125 mm h^{-1}, and c) 125–225 mm h^{-1}.

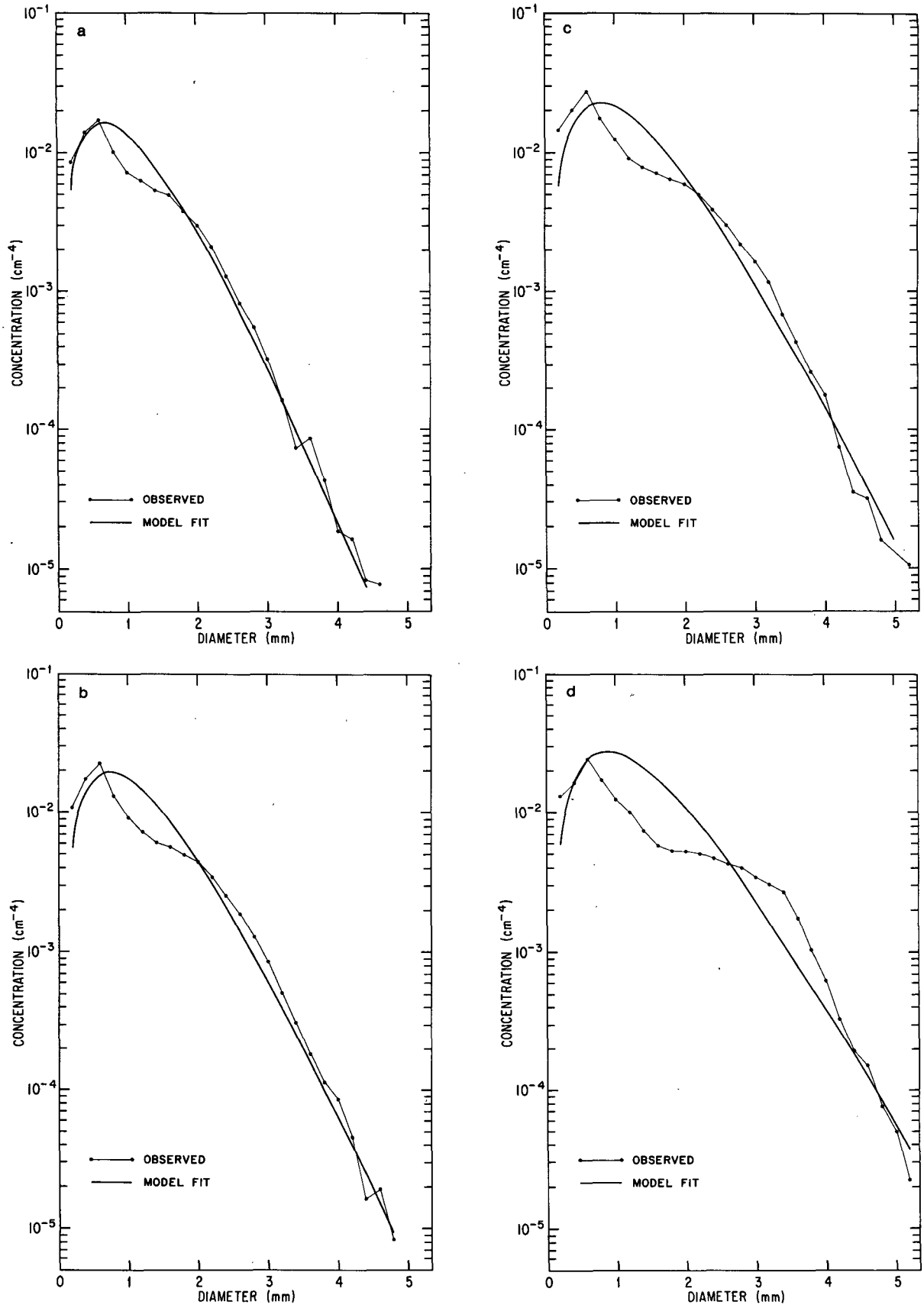

FIG. 3. Mean drop-size distributions from observations at 450 m altitude, and Γ-function fit, for rain rates: a) 25–62.5 mm h^{-1}, b) 62.5–125 mm h^{-1}, c) 125–225 mm h^{-1}, and d) >225 mm h^{-1}.

The drop-size distributions presented in MIL-STD-210B (Department of Defense 1973) are based upon an exponential model of drop-number concentrations. Numerous investigators have pointed out the inadequacies of the exponential distribution in describing observed drop-size distributions (e.g., Ulbrich 1983), particularly for high-intensity convective rains. As part of this study we examined the feasibility of using an exponential fit with a constant slope parameter to model the high rain rate data sample studied herein. Although the results of this exercise were not positive enough to warrant use of this approach to model the data, these results are presented in the Appendix.

The Γ-distribution function, of which the exponential is a special case, fits tropical convective-rain distributions particularly well (Willis 1984). Although a log-normal distribution (Feingold and Levin 1986) is also a candidate, the fits provided by the two distributions should not differ significantly. The Γ overcomes the deficiencies of the exponential in fitting observed data, yet is related to the exponential, is versatile, and easy to use.

Numerous authors (e.g., Ulbrich 1983) have used the modified Γ-distribution given by the following expression:

$$N(D) = N_G D^{\alpha} e^{-\Lambda D}. \tag{1}$$

Here D is the drop diameter, $N(D)dD$ the concentration of drops having diameters between D and $D + dD$, N_G the concentration parameter, Λ the slope parameter, and α the curvature parameter. When the curvature parameter in Eq. (1), α, is zero, the gamma reduces to the exponential Γ-distribution function.

This Γ-distribution function is the basis for the proposed model fit to the new high-intensity rainfall dataset. The proposed drop-size–distribution model consists of two parts: 1) the Γ-function fit to the normalized data set of Fig. 4 (combined dataset for all altitudes), and 2) an empirically determined relationship between water content, M, and median volume diameter, D_0, as described by Willis (1984). To fit an individual distribution, all that need be specified is the water content, M, or the rainfall rate, R. The fit to an individual distribution is then determined by what amounts to a denormalization of the fit to the entire normalized sample.

The model is applied as follows. If a drop-size distribution is desired for a given liquid-water content M (g m^{-3}), first compute the median volume diameter from the following empirical relationship

$$D_0 = 0.1571 M^{0.1681}, \tag{2}$$

where D_0 is in centimeters (Willis 1984). Or, alternatively, if the rainfall rate, R (mm h^{-1}) is specified, first compute M from

$$M = 0.062 R^{0.913}. \tag{3}$$

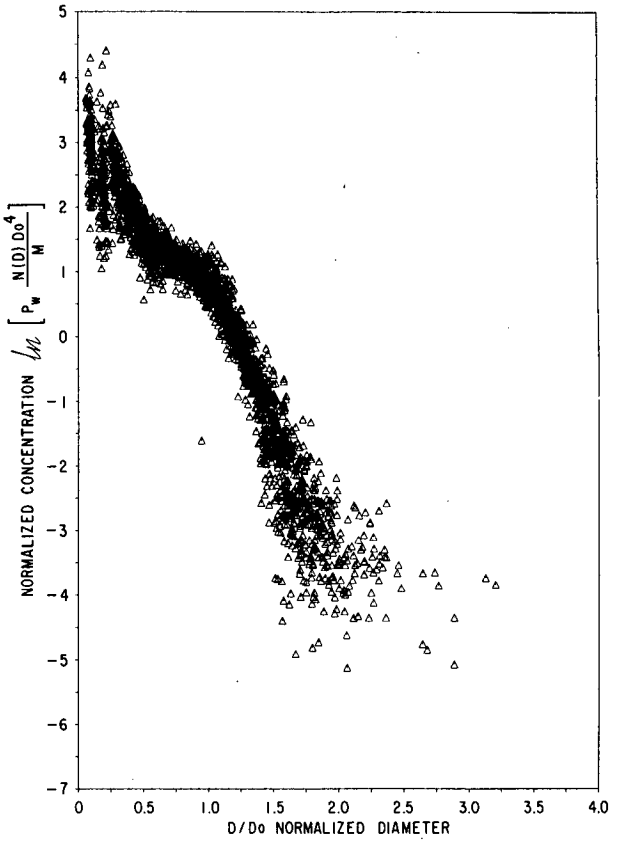

FIG. 4. Normalized distribution of the total data sample.

Once the median volume diameter has been determined, then the three parameters of the Γ-distribution, Eq. (1), needed for the model are computed from the following three relationships based on the fit to the normalized dataset:

$$\Lambda = 5.5880/D_0 \tag{4}$$

$$\alpha = 2.160 \tag{5}$$

$$N_G = \frac{512.85 M \times 10^{-6}}{D_0^4}\left(\frac{1}{D_0}\right)^{2.160}. \tag{6}$$

As an example, the equations for the drop-size distributions for the five representative rainfall rates discussed in section 2 are derived. For each rainfall rate D_0, Λ, α, and N_G were calculated from Eqs. (2), (4), (5) and (6), respectively. The resulting equations are:

$$36 \text{ mm/hr} \quad N(D) = 45.08 D^{2.160} e^{-32.75D} \tag{7}$$

$$84 \text{ mm/hr} \quad N(D) = 43.86 D^{2.160} e^{-28.76D} \tag{8}$$

$$168 \text{ mm/hr} \quad N(D) = 42.88 D^{2.160} e^{-25.86D} \tag{9}$$

$$432 \text{ mm/hr} \quad N(D) = 41.59 D^{2.160} e^{-22.37D} \tag{10}$$

$$1872 \text{ mm/hr} \quad N(D) = 39.66 D^{2.160} e^{-17.86D}. \tag{11}$$

c. Goodness of fit

In Figs. 1, 2 and 3, the model fit is compared with stratified subsets of the data on which it is based. The fits are visually quite good for this dependent data. The squared error was computed at each observation point by:

$$SE = [\log N_i(\text{obs.}) - \log N_i(\text{fit})]^2. \quad (12)$$

The squared errors were summed over equal intervals from $D = 0.2$ mm ($i = 1$) to $D = 5.2$ mm ($i = 26$) and the resultant total squared errors are presented in Table 1 for the same stratifications of the dependent data set used in Fig. 1–3. To find the average error these total errors should be divided by $n = 26$. The errors of the Marshall-Palmer distribution fit to the data are included in Table 1 for comparison. The errors computed from the log-transformed values are used here for computing the squared errors because this gives a good measure of the fit to the overall distribution. If the errors are computed from the raw spectral densities, the total squared error is dominated by the goodness of fit at the first few small diameters and is meaningless as a measure of fit to the overall shape of the distribution.

For the data collected at the low sampling altitude (450 m), the overall fit is good, but the bimodal tendency noted in the most intense low-level distributions does not lend itself well to a simple functional fit. Consequently, the error is higher at these extreme rainfall rates. Shiotsuki (1976) presents several intense-rainfall distributions that support this spectral shape for intense rainfall at the surface.

The observed differences in the spectra with altitude are discussed in section 3a. The Mueller and Sims data, taken at the surface and discussed subsequently, are similar to the new spectra observed aloft. These surface distributions tend to have lower number densities of drops of $D < 1$ mm than the distributions measured aloft. Also, it should be noted that significant evaporation below cloud base could considerably alter the surface distributions from those observed aloft.

TABLE 1. Total squared error of model fit to observed data (mean spectrum). SE is computed as the difference of the $\log_{10}$ of the observed and fit values, and summed from 0.2 mm to 5.2 mm ($N = 26$). Data groupings and stratifications are as in Figs. 1–3.

	Rain rate (mm h^{-1})	Model	Marshall–Palmer
All Data	25.0–62.5	0.44	4.04
	62.5–125.	0.45	2.41
	125.–225.	0.93	3.40
	>225.	1.75	1.97
	Mean	0.89 (0.034)	2.96 (0.114)
3-km Altitude	25.0–62.5	1.04	4.04
	62.5–125.	0.52	2.87
	125.–225.	1.99	4.35
0.45 km Altitude	25.0–62.5	0.67	4.07
	62.5–125.	2.02	6.43
	125.–225.	1.63	5.18
	>225.	1.72	2.69

TABLE 2. Total squared error of model fit to observed independent data (mean spectra) of Mueller and Sims (1966). SE is computed as the difference of the $\log_{10}$ of the observed and fit values, and summed from 0.5 mm to 5.0 mm ($N = 46$). Data stratifications are as in Figs. 5–9.

Location	Rain rate (mm h^{-1})	Model	Marshall–Palmer
Miami	106	4.19	4.38
	212	0.41	2.42
	429	1.84	4.16
Majuro	115	3.77	7.69
	171	2.83	7.54
Bogor	125	1.86	3.66
	180	2.54	7.58
Island Beach	101	3.19	5.74
	148	7.24	11.76
Franklin	144	5.05	11.72
	205	4.34	9.64
	Mean	3.39 (0.074)	6.94 (0.151)

We now examine how well this model fits the independently observed high-rainfall-rate data from Mueller and Sims (1966) gathered at Miami, Majuro Atoll, Bogor, New Jersey, and North Carolina. Total squared errors for these model fits, summed over equal intervals from $D = 0.5$ to 5.0 mm ($n = 46$), are presented in Table 2. Keep in mind that the model fit is not a tailored statistical fit to each individual spectrum. The only input specified is either the rainfall rate or the water content. The mean squared error (log) is about twice that of the dependent dataset. Much of this is due to the fit for small drops ($D < 1$ mm) in this surface data. The Marshall-Palmer error is also higher for this reason.

Fig. 5 shows the fit to average distributions for three categories of rainfall rate for Miami, Florida. Visually the fits to these three spectra are quite good. The fit is particularly good for the two highest-rate categories of 212 and 429 mm h^{-1}. Fig. 6 presents the fit for average spectra from Majuro Atoll in the tropical Pacific for mean rain rates of 115 and 171 mm h^{-1}. Visually the fits are good, particularly for the 115 mm h^{-1} rate spectrum. The same is true for the data from Bogor, Indonesia, (Fig. 7), but the model underestimates the number concentration of drops near 1.5 mm diameter at the 180 mm h^{-1} rate.

Figs. 8 and 9 display the fit for the highest-rate categories for two locations with more continental characteristics. The fit is generally quite good, but the model underestimates the concentrations at $D = 1.5$ mm and slightly overestimates the concentrations of the largest drops. The Marshall-Palmer fit ($N_0 = 0.08$ cm^{-4}) for these four mean rainfall rates (not shown) severely underestimates concentrations at $D = 1.5$ mm and se-

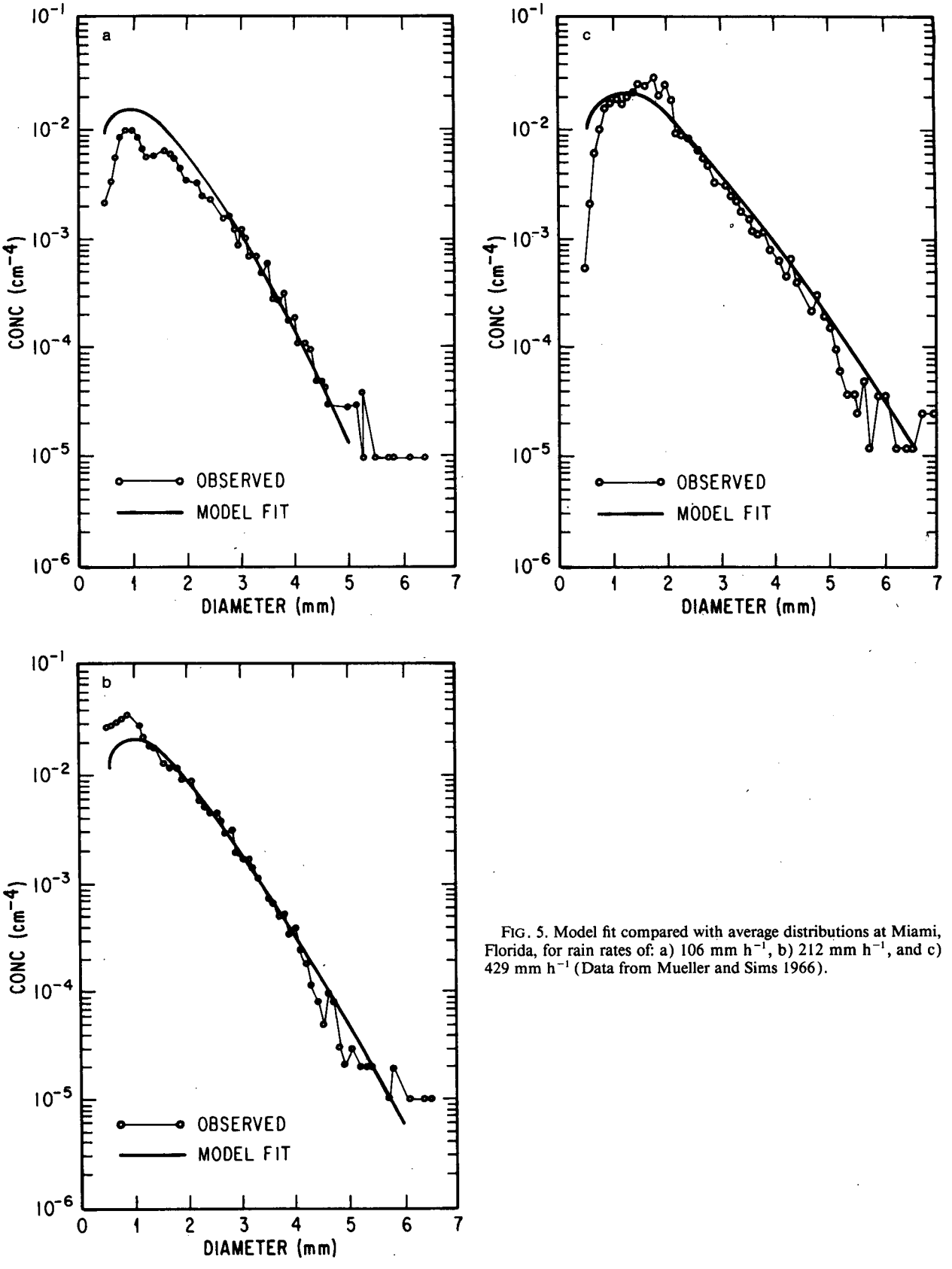

FIG. 5. Model fit compared with average distributions at Miami, Florida, for rain rates of: a) 106 mm h^{-1}, b) 212 mm h^{-1}, and c) 429 mm h^{-1} (Data from Mueller and Sims 1966).

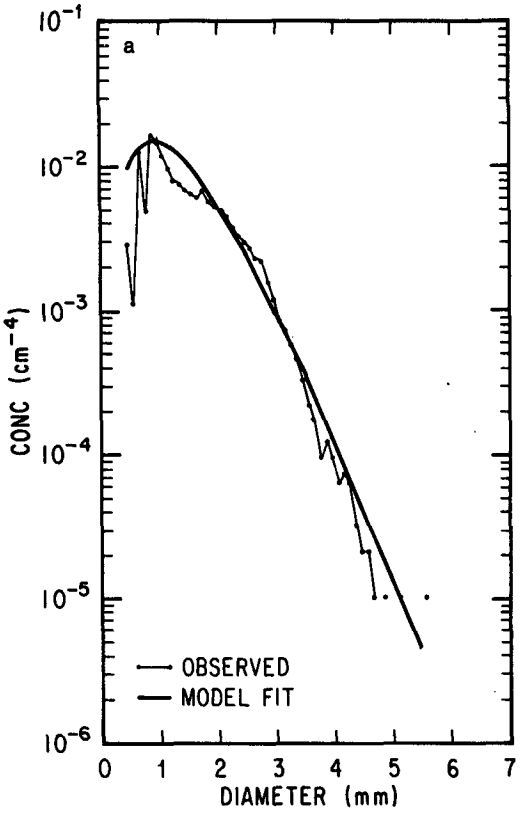

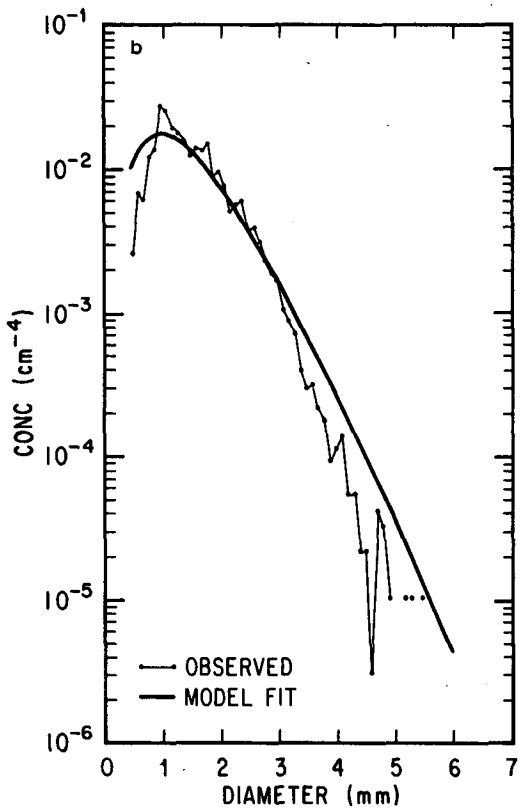

FIG. 6. Model fit compared with average distributions at Majuro Atoll, tropical Pacific, for rain rates of: a) 115 mm h^{-1}, and b) 171 mm h^{-1} (Data from Mueller and Sims 1966).

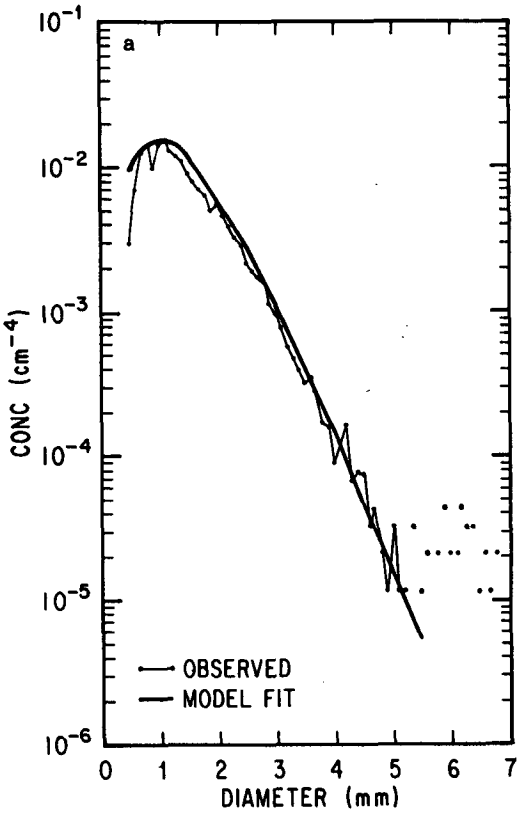

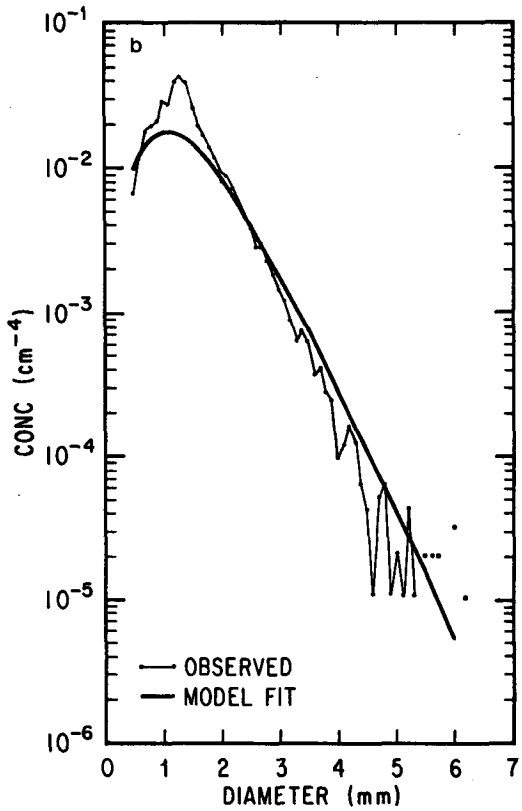

FIG. 7. Model fit compared with average distributions at Bogor, Indonesia, for rain rates of: a) 125 mm h^{-1}, and b) 180 mm h^{-1} (Data from Mueller and Sims 1966).

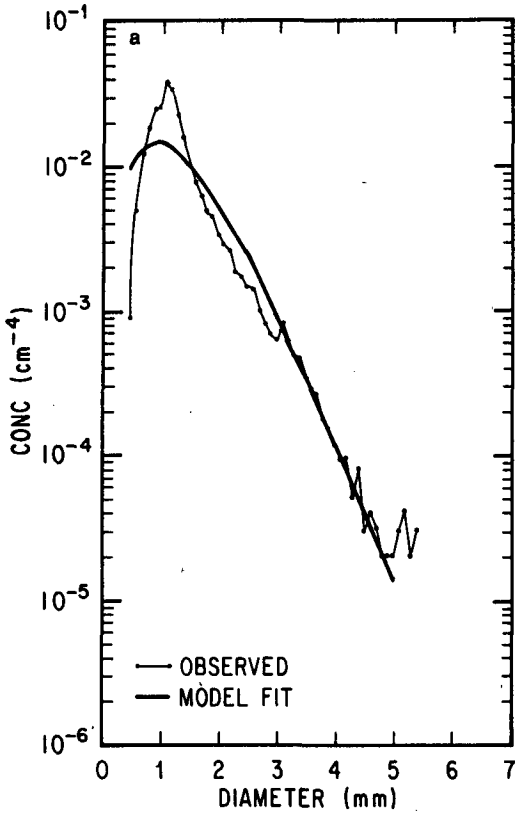

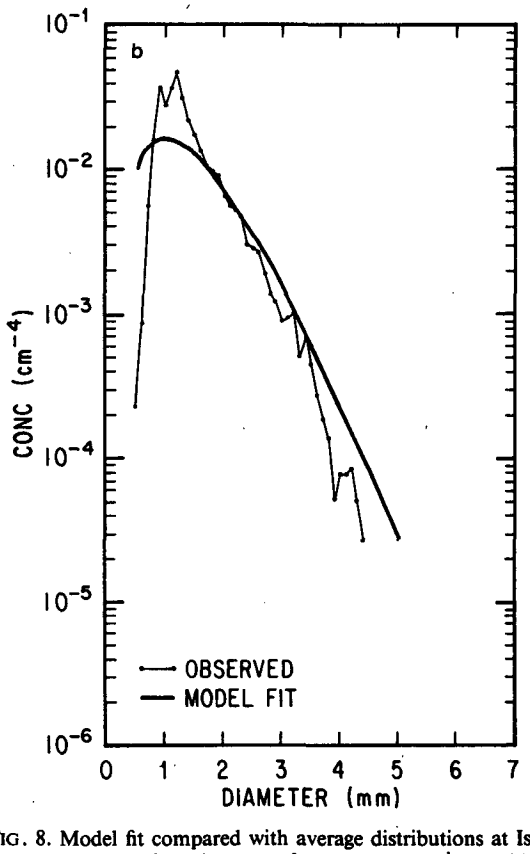

FIG. 8. Model fit compared with average distributions at Island Beach, New Jersey, for rain rates of: a) 101 mm h^{-1}, and b) 148 mm h^{-1} (Data from Mueller and Sims 1966).

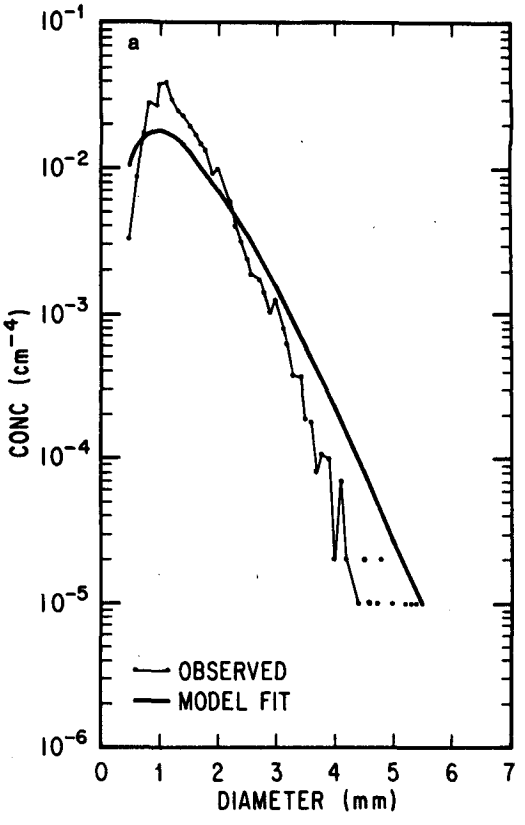

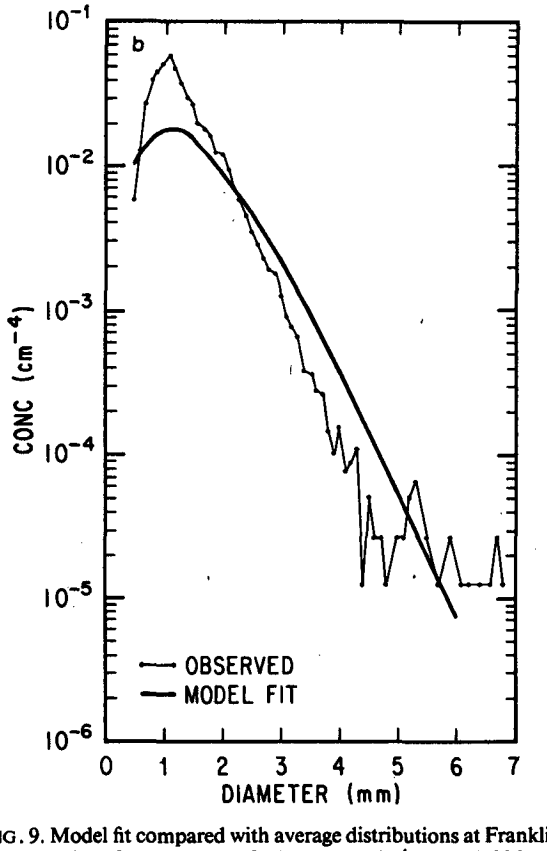

FIG. 9. Model fit compared with average distributions at Franklin, North Carolina, for rain rates of: a) 144 mm h^{-1}, and b) 205 mm h^{-1} (Data from Mueller and Sims 1966).

verely overestimates the concentrations at $D > 4$ mm. Overall, the Γ-distribution model fits this independent set of high-rainfall-rate data quite well, particularly for locations within the tropics.

There are indications that the Γ-fit model may break down for very extreme rates, such as the 1 min world record 1872 mm h^{-1}, due to the tendency for these distributions to become bimodal. However, based on the generally excellent fits of the model to the independent dataset, as well as the dependent data, use of the model up to the world record 1-h rate of 432 mm h^{-1} is justified.

4. Liquid water content

Section 2 discussed extreme rainfall rates at the surface. This section addresses extremes of precipitation water content aloft. The liquid-water content contained in precipitation size drops can be computed from the drop-size distribution, as well as the rainfall rate. This mass of water per cubic meter of air space is important for many applications and actually is a more fundamental parameter of the distributions than the rainfall rate. It is related to the rainfall rate, since R and M are proportional to $\Sigma v D^3$ and ΣD^3, respectively. The drop terminal velocity (v) is not a strong function of drop diameter, particularly at large diameters. For applied problems there is considerable interest in extremes of liquid water content aloft. Extreme values of liquid-water content in convective storms are nearly always dominated by the precipitation water content, and not the cloud-droplet water content. Thus, liquid-water content is an appropriate topic in a study of drop-size distributions.

Measurements of liquid-water content (M) in severe convective storms have not been made on a systematic basis (Grantham et al. 1983). However, a value as high as 44 g m^{-3} was reported by Roys and Kessler (1966). Their aircraft observations of maximum values in Oklahoma thunderstorms show that the next highest value was about 14 g m^{-3}, and the average of maximum amounts in 28 aircraft passes, including the 44 g m^{-3} value, was 8.4 g m^{-3}. Kyle and Sand (1973) found total condensed-water content of about 20 g m^{-3} in "High Plains" thunderstorms. Mueller and Sims observed peak 10.5-s rainwater-content values of 22 and 29 g m^{-3} at the surface in Miami.

Extreme values of rain-water content, and rain rate, have been found to be fairly well described by a log-normal distribution. Such a distribution for the total sample of hurricane–tropical storm data analyzed for this study, and the individual sample for Hurricane Eloise (1965) are shown in Fig. 10. The ordinate is the conditional probability that a given M is exceeded (i.e., in a sample where $R > 0$). About 1% of the almost 14 000 10-s aircraft-track samples had a value of $M > 4$ g m^{-3}. For comparison, the distributions for surface data from Mueller and Sims are also shown, as are the Roys and Kessler data (excluding the 44 g m^{-3} value). Note that the Roys and Kessler data are for maximum water content within Oklahoma thunderstorms. The Mueller and Sims data cover a 1 yr period at Miami, Florida; Franklin, North Carolina; and Majuro Atoll. The data for Bogor, Indonesia, was omitted for clarity, as it coincides with the distribution of the data from this study. All of the distributions are very close to the data samples of this study, except possibly Miami, where the slope is the same but the curve is shifted. Note that the Roys-and-Kessler distribution changes quite radically at about 5 g m^{-3}, and its high water-content values exhibit a significantly different slope than the data of this study and the Mueller and Sims data. Keep in mind that these data were sampled at the −30°C level in Oklahoma thunderstorms. At this level in these storms they could have been looking at accumulations of graupel, and not simply rain water content. This could explain the slope and the departure from log normality.

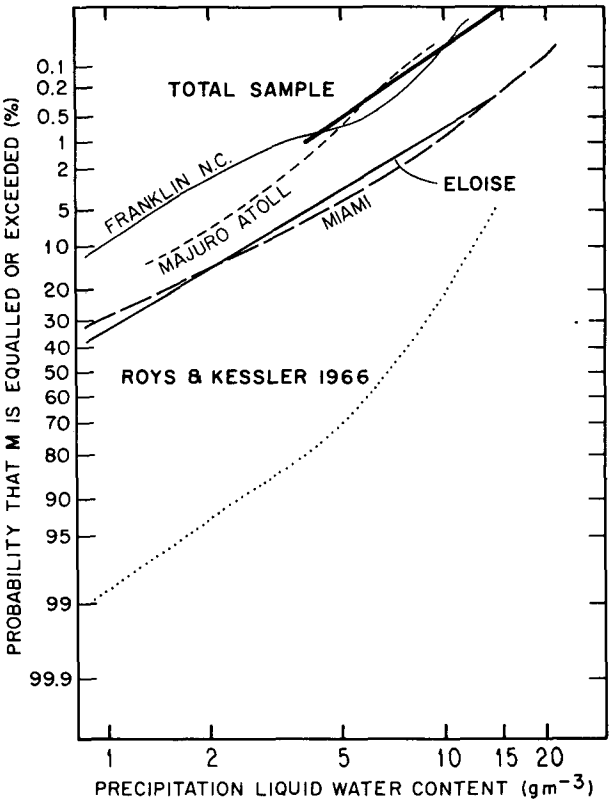

FIG. 10. Conditional probability ($R > 0$) of a given precipitation water content being exceeded. A straight line indicates that distribution is log-normal.

5. Summary

A large sample of drop-size distributions from intense rainfall in tropical convection was analyzed. A Γ-distribution function was fit to the normalized set of intense-rainfall drop-size distributions. This fit

formed the basis of a model distribution as a function of rainfall rate of precipitation water content. The model fit was applied to numerous observed high–rainfall-rate drop-size distributions from several geographic locations and was found to very reasonably characterize these observed distributions. The distributions in heavy rain are essentially similar over a wide range of geographic locations, both tropical and continental.

This model was used to specify the profiles of drop-size distributions for five categories of intense rainfall. The additional data considered in this study provide an improved specification of drop-size distributions for intense rainfall. In the sample of airborne data there appears to be some difference in the distributions from 3000 m altitude and those much nearer the surface at 450 m. Additional data are needed to determine the precise nature and extent of this difference.

Acknowledgments. The authors are grateful to the flight crews of the NOAA Office of Aircraft Operations who made the data collection possible, Major Al Boehm, AFGL, for his helpful suggestions, to Ms. Joyce O. Berkeley, NOAA, for reducing the rain rate data, and to Mrs. Helen Connell, AFGL, for typing the report.

APPENDIX

Examination of a Constant Slope Exponential Fit

There is some observational and theoretical evidence in support of a constant value of λ (exponential-fit slope parameter) for higher rainfall rates (Eq. 1 $\alpha = 0$). Consequently this fit was examined as a potential model for this high–rain-rate dataset. Even though the distributions are better fit by a Γ distribution, it is of interest to examine the relationship between the total

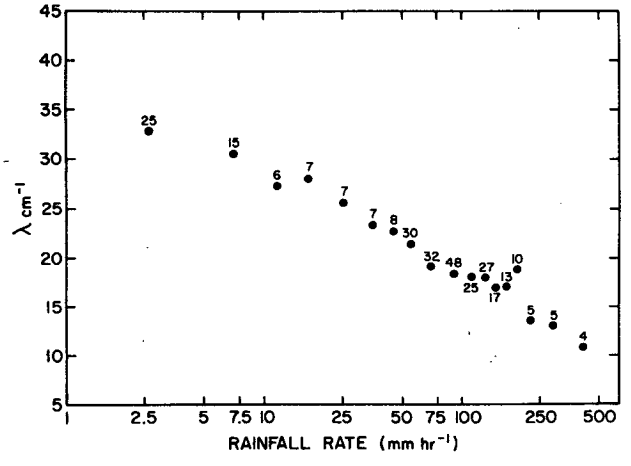

FIG. 11. Values of slope parameter for exponential fits to average distributions ($D > 1$ mm) plotted against rainfall rate (total new tropical convection-data sample). Numbers indicate number of distributions in each class interval of rainfall rate.

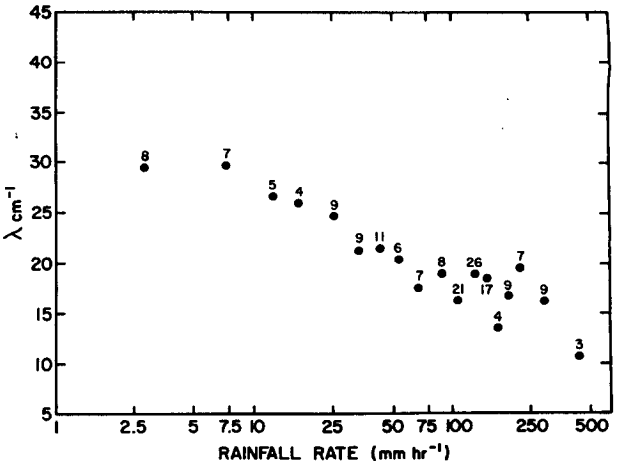

FIG. 12. Values of slope parameter for exponential fit to average distributions ($D > 1$ mm) plotted against rainfall rate–total Mueller-and-Sims high-dataset. Numbers indicate number of distributions in each class interval of rainfall rate.

number of drops and the slope of the exponential distribution fit to observed spectra. At high rainwater contents, the raindrop-size distribution is controlled primarily by the processes of coalescence and collision breakup. Pasqualucci (1982) found that for water contents > 1.2 g m^{-3} the slope parameter of an exponential fit λ becomes constant and independent of M, while N_0 continues to increase with increasing M. Recently, Hodson (1986) found that for $R > 25$ mm h^{-1}, λ was constant at 21–23 cm^{-1}. Here we examine the new dataset, as well as the data of Mueller and Sims (1966) for an exponential-fit λ constant and independent of R.

The entire high–rainfall-rate dataset was bin-averaged within class intervals of rainfall rate. Since this dataset emphasized high–rate data, a random sample of lower–rainfall-rate data from the same storms has been included to complete the dataset. Slope parameters from a least squares exponential fit to these resulting mean spectra are plotted against rainfall rate in Fig. 11. These data show an overall trend of decreasing slope (λ) with increasing rainfall rate. However, there is an inflection at 90 mm h^{-1}, and λ remains nearly constant from there to 200 mm h^{-1}. But, the 3 highest data points then clearly indicate a decreasing λ as R is increased further. This could be due to sampling error, but, these three points represent 14 individual distributions. Remember that these extremely high rate spectra tend towards bimodality, as previously discussed, and thus will have a very flat exponential slope from a least-squares fit. But, when an alternate exponential fitting method is applied (the analytical exponential of Willis (1984)), the data show an even more consistent decrease of λ with increasing rainfall rate. These data, which include a large sample of high-rainfall rates associated with convection, do not support a

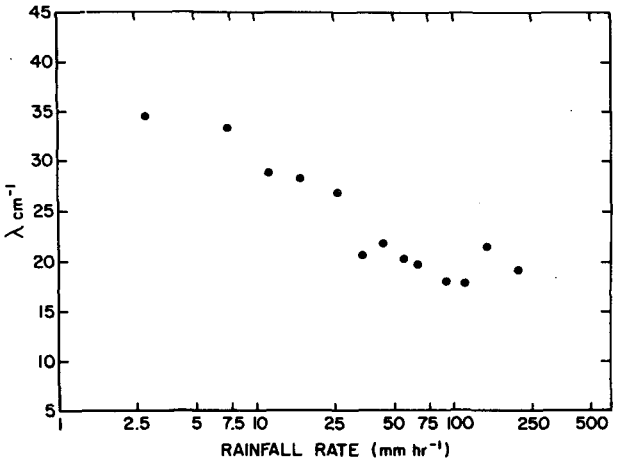

FIG. 13. Values of slope parameter for exponential fit to average distributions plotted against rainfall rate–Franklin, North Carolina mean distributions.

constant exponential distribution slope at rainfall rates above 25 mm hr^{-1}. However, the relationship between the slope of the exponential fit and the rainfall rate does change at 90 mm hr^{-1}.

Fig. 12 summarizes a similar analysis of the nearly complete Mueller and Sims combined datasets for Franklin, North Carolina; Bogor, Indonesia; Majuro Atoll; and Miami, Florida. As in Fig. 11, the overall trend is clearly one of decreasing λ with increasing R. However, there is an inflection at about 75 mm h^{-1}, and it is somewhat ambiguous after this point as to whether λ continues to decrease, or remains constant. It is almost as if there are two parts to the curve. Sampling becomes a factor for the highest-rate categories, which contain fewer individual spectra. Our interpretation of the results in Fig. 12 differs from Hodson (1986) who states that all of the results of Mueller and Sims (1966) show that for rainfall rates > 25 mm h^{-1}, the average value of λ at each site lies between 22–23 cm^{-1}. He indicates that the value of λ is nearly constant for R > 25 mm h^{-1}, which is inconsistent with the results of Fig. 11. And further confusing the issue, Mueller and Sims (1966) state that, for Miami, the λ remains nearly constant, or even increases slightly with increasing rainfall rate.

When treated individually, the datasets do show a slightly greater tendency towards a constant λ. For example, Fig. 13 presents the data for the mean distributions from Franklin, North Carolina. There is considerable scatter, and an inflection could be interpreted as occurring at either 30 or 90 mm h^{-1}. A linear, least-squares fit of the data points would clearly support a decreasing λ to 100 mm h^{-1}. The data in this figure are bin averages of Mueller and Sims mean spectra within the same intervals of R used in Figs. 11 and 12. The analysis of individual location datasets tends to support Hodson's contention of a constant λ for R > 25 mm h^{-1} more than the combined datasets. However, there is considerable scatter and the results are inconclusive. Based on the new dataset and the analysis of the combined Mueller and Sims data, we conclude that the distributions tend towards a slope that continues to decrease with increasing rainfall rate, and that if there is a tendency towards a constant exponential-slope parameter it occurs at a rainfall rate nearer to 100 mm h^{-1}.

REFERENCES

Blanchard, D. C., and A. T. Spencer, 1970: Experiments on the generation of raindrop-size distributions by drop breakup. *J. Atmos. Sci.*, **27**, 101–108.

Department of Defense, 1973: Military Standard, Climatic Extremes for Military Equipment. MIL-STD-210B, 72 pp. [Available from the Office of the Under Secretary of Defense, Research and Engineering, Washington DC.]

Feingold, G., and Z. Levin, 1986: The lognormal fit to raindrop spectra from frontal convective clouds in Israel. *J. Climate Appl. Meteor.*, **25**, 1346–1363.

Grantham, D. D., et al., 1983: Water vapor, precipitation, clouds and fog. *Handbook of Geophysics and Space Environments*, Chapter 16, 1983 revision, AFGL-TR-83-0181, 141 pp.

Hodson, M. C., 1986: Raindrop size distribution. *J. Climate Appl. Meteor.*, **25**, 1070–1074.

Hudson, N. W., 1963: Raindrop size distribution in high intensity storm. *Rhodesian J. Agric. Res.*, **1**, 6–11 (quoted in Blanchard and Spencer, 1970)

Jorgensen, D. P., and P. T. Willis, 1982: A *Z–R* relationship for hurricanes. *J. Appl. Meteor.*, **21**, 356–366.

Knollenberg, R. G., 1981: *Techniques for Probing Cloud Microstructure: Clouds, Their Formation, Optical Properties and Effects.* P. V. Hobbs and A. Deepak, Eds., Academic Press, 15–92.

Kyle, T. G., and W. R. Sand, 1973: Water content in convective storm clouds. *Science*, **180**, 1274–1276.

Marshall, J. S., and W. McK. Palmer, 1948: The distribution of raindrops with size. *J. Meteor.*, **5**, 165–166.

Mueller, E. A., and A. L. Sims, 1966: Radar Cross Sections from Drop Size Spectra. Tech. Rep. ECOM-00032-F, Contract DA-28-043 AMC-00032 (E) Illinois State Water Survey, Urbana, 110 pp. [AD-645218.]

Pasqualucci, F., 1982: The variation of drop size distribution in convective storms: A comparison between theory and measurement. *Geophys. Res. Lett.*, **9**, 839–841.

Roys, G. P., and E. Kessler, 1966: Measurements by Aircraft of Condensed Water in Great Plains Thunderstorms. ESSA Tech. Note 49-NSSP-19, 17 pp.

Sekhon, R. S., and R. C. Srivastava, 1970: Snow size spectra and radar reflectivity. *J. Atmos. Sci.*, **27**, 299–307.

——, and ——, 1971: Doppler observations of drop size distributions in a thunderstorm. *J. Atmos. Sci.*, **28**, 983–994.

Shiotsuki, Y., 1976: An estimation of drop-size distribution in severe rainfall. *J. Meteor. Soc. Japan*, **54**, 259–263.

Tattelman, P., and K. G. Scharr, 1983: A model for estimating one-minute rainfall rates. *J. Climate Appl. Meteor.*, **22**, 1575–1580.

——, and D. D. Grantham, 1983a: *Northern Hemisphere Atlas of 1-Min Rainfall Rates.* AFGL-TR-83-0267, 81 pp. [ADA145411.]

——, and ——, 1983b: *Southern Hemisphere Atlas of 1-Min Rainfall Rates.* AFGL-TR-83-0285, 81 pp. [ADA145421.]

Ulbrich, C. W., 1983: Natural variations in the analytical form of the raindrop size distribution. *J. Appl. Meteor.*, **22**, 1764–1775.

Valdez, M. P., and K. C. Young, 1985: Number fluxes in equilibrium raindrop populations: A Markov chain analysis. *J. Atmos. Sci.*, **42**, 1024–1036.

Willis, P. T., 1984: Functional fits to some observed drop size distributions and parameterizations of rain. *J. Atmos. Sci.*, **41**, 1648–1661.